

# On the motifs distribution in random hierarchical networks

V.A. Avetisov<sup>1</sup>, S.K. Nechaev<sup>2,3,4</sup>, A.B. Shkarin<sup>5</sup>

<sup>1</sup>*N.N. Semenov Institute of Chemical Physics of the Russian Academy of Sciences, 119991, Moscow, Russia*

<sup>2</sup>*LPTMS, Université Paris Sud, 91405 Orsay Cedex, France*

<sup>3</sup>*P.N. Lebedev Physical Institute of the Russian Academy of Sciences, 119991, Moscow, Russia*

<sup>4</sup>*J.-V. Poncelet Laboratory, Independent University, 119002, Moscow, Russia*

<sup>5</sup>*Moscow Physical-Technical Institute, 141700, Dolgoprudnyj, Moscow district, Russia*

(Dated: October 13, 2018)

The distribution of motifs in random hierarchical networks defined by nonsymmetric random block-hierarchical adjacency matrices, is constructed for the first time. According to the classification of U. Alon *et al* of network superfamilies [11] by their motifs distributions, our artificial directed random hierarchical networks falls into the superfamily of natural networks to which the class of neuron networks belongs. This is the first example of “handmade” networks with the motifs distribution as in a special class of natural networks of essential biological importance.

## I. INTRODUCTION AND BASIC DEFINITIONS

Most commonly, the hierarchy of states emerges in many-particle systems of various origins with a large number of “frozen” constraints with different scales, which generate multidimensional hypersurfaces of potential energy (or free energy) with an astronomically large number of local minima. Typical examples of such systems (often referred to as complex systems) are glasses and globular proteins. The hierarchical concept applied to such systems presumes that local minima of the energy landscape are clustered into hierarchically embedded basins of minima. Namely, each large basin consists of smaller basins each of which in turn contains embedded still smaller basins, and so on. Local minima basins are separated from one another by hierarchically ordered barriers (the smaller the basins, the “lower” the barriers separating them).

Apart from the dynamic contents of the hierarchical concept, the determination of the hierarchical organization of “ultrametric phase spaces” in the observed statistical regularities is of considerable interest. A visual example of the such a structural organization is the so-called crumpled globule discussed for the first time in [1]. The thermodynamically equilibrium spatial configuration of such a globule resembles the Peano curve [2] embedded into a 3D space. Spatial packing of a crumpled globule can be represented schematically by a single folded motive reproduced on a growing scale. The hierarchical packing naturally leads to a block-hierarchical network of contacts between the links of a chain described by a block-hierarchical matrix of contacts. Naturally, the presence of inhomogeneities in the hierarchy of crumples introduces randomness in the block-hierarchical network of contacts, which requires the determination of statistical characteristics of an ensemble of random block-hierarchical matrices of contacts. In recent works [3, 4] we have considered statistical properties of random hierarchical networks defined by adjacency matrices in form of block-hierarchical Parisi matrix [5]. Remind that a

network is a set of vertices (or nodes) and connections between them (links or edges). We suppose that in the network there are no any self-connections and multiple edges. The network is random if any link occurs with a certain probability. The network is directed if any link either has an orientation ( $i \rightarrow j$ ) or is bidirectional ( $i \leftrightarrow j$ ). Otherwise the network is non-directed.

The investigation of statistical properties of random graphs and networks implies studying of spectral properties of their adjacency matrices (e.g. [6, 7]), the same question can be posed for block-hierarchical networks. It was found in [3, 4] that the spectral density of adjacency matrices has power law (“heavy”) tails, typical for scale-free networks. This observation has been supplemented by direct investigations of such typical statistical properties of networks as vertex degree distribution, which turned out to be abnormally wide (but not scale-free). Hence following the conventional classification (e.g. [8]), random hierarchical networks could be attributed to the class of scale-free (according to the spectral density) or polyscale (according to the vertex degree distribution) networks.

Scale-free networks are associated with a variety of structures and systems, such as protein folding and biopolymer dynamics; cell metabolism; neural, information and communication networks; various evolutionary, ecological, social and economical systems. Statistical characteristics of many natural networks are described in the review [8]. Because of wide usage of a “network paradigm” it seems quite natural that a “handmade” design of artificial networks with some observed statistical characteristics close to that of natural networks is of primary importance. Such a design might be very useful tool for searching for the correlations between the network structural organization and the functions.

Until recently building of scale-free networks was based in almost all works on a step-by-step growing process based on the preferential attachment method [9] and its various modifications. In these approaches the new vertices are connected to the existing ones with proba-

bility which depend on their current vertex degree. Most of the statistical characteristics of artificial scale-free networks including spectral distribution of adjacency matrix were obtained for networks built in this way. It should be noted that the preferential attachment process, which realizes locally inhomogeneous *vertex* grouping, implicitly implies some mechanisms controlling the current state of a network with long-term “evolutionary memory”.

Unlike the preferential attachment-like methods, building of hierarchical networks is based on constructing of hierarchically embedded clusters of *links*. The configuration of links is usually described by an adjacency matrix  $A$  in which for matrix elements  $a_{ij}$  one has  $a_{ij} = 1$  if there is a link connecting nodes  $i$  and  $j$  and  $a_{ij} = 0$  otherwise. Adjacency matrix  $A$  for non-directed graph is symmetric, i.e.  $a_{ij} = a_{ji}$ . To the contrary, for the directed network  $a_{ij} = 1$  and  $a_{ji} = 0$  for the oriented link  $i \rightarrow j$  and  $a_{ij} = a_{ji} = 1$  for the bidirectional one  $i \leftrightarrow j$ . Therefore the generic adjacency matrix  $A$  is not necessarily symmetric.

It is known that the classification of many natural networks according to their vertex degree distribution, or clustering coefficient is too rough and does not provide any relevant information about the internal network structure. Much more detailed information about the network structure can be provided by investigating the local topological characteristics, the so-called *motifs* and their distributions [10, 11]. For example, it is known that all networks, according to their three-vertex oriented motifs distribution, can be divided into four *superfamilies* [11].

In this letter we announce the results of the investigation of motifs distribution in random hierarchical networks. The key outcome consists in the fact that the motifs distribution of random block-hierarchical networks clearly falls into one of the universal superfamilies, which includes, in particular, networks of neurons. Besides, we claim the existence of a phase transition (in respect to motifs’ distribution) in an ensemble of block-hierarchical networks in the thermodynamic limit.

## II. DISTRIBUTION OF MOTIFS IN HIERARCHICAL NETWORKS

Remind that local topological properties of networks, both directed and non-directed, for given number of vertices and vertex degree distribution can be characterized by the rates of connected subgraphs. Since the number of such subgraphs grows combinatorially with their size, usually only small subgraphs are considered. In particular, in the works [10, 11] only subgraphs of size 3 (triads) were analyzed for directed networks. There are 13 different configurations of such triads. They all are enumerated in the Fig.1.



Figure 1: Connected subgraphs-triads for directed networks.

The rates of subgraphs in a given network depend on the vertex degree distribution. This complicates the comparison of networks of different sizes and different vertex degree distributions by the rates of their subgraphs. In order to compensate these differences, the procedure of so-called *network randomization* was proposed in works [10, 11]. In this procedure the network experiences multiple permutations of links under the condition of conservation in each vertex of the number of incoming, outgoing and bidirectional links. Using this method an ensemble of randomized versions of a given network is generated, and for every subgraph the *statistical significance*

$$Z_k = \frac{N_k - \langle N_k \rangle_{\text{rand}}}{\sigma_k} \quad (1)$$

is calculated, where  $N_k$  is the amount of  $k$ -th subgraphs in the initial network and  $\langle N_k \rangle_{\text{rand}}$  and  $\sigma_k$  are correspondingly the mean and the standard deviation of  $N_k$  for the randomized networks. Subgraphs with the statistical significance essentially exceeding 1 are called *motifs* [10]. The motifs’ distribution of the network under consideration is characterized by a *significance profile* which is a normalized vector

$$\mathbf{p} = \{p_1, \dots, p_m\} \quad (2)$$

of statistical significance for all subgraphs of given size. The components of the vector  $\mathbf{p}$  are:

$$p_k = \frac{Z_k}{\sqrt{\sum_{k=1}^m Z_k^2}} \quad (k = 1, \dots, m) \quad (3)$$

It has been demonstrated in the papers [10, 11] that significance profile distribution could be used to divide networks into superfamilies. For directed networks only 4 of such superfamilies were determined. The networks with considerably different functional properties, for example, the neuron networks and transcriptional networks in unicellular organisms, belong to different superfamilies. In [10, 11] also the undirected networks were classified according to their tetradic motifs. These networks were separated in four superfamilies as well.

It is interesting that artificial random scale-free networks generated by the preferential attachment method form a separate superfamily which does not coincide with any superfamily of real networks. In the Fig.2 we have reproduced from [11] the significance profiles of one of the superfamilies for directed networks, which later on will be compared with our results on the distribution of motifs in the block-hierarchical random networks.



each value of  $\mu$  the significance profiles are averaged over an ensemble of corresponding random hierarchical networks. The typical distributions of motifs for directed hierarchical networks is shown in Fig.4. As one can see, the distributions for different values of  $\mu$  look very similar and are not too sensitive to the concrete value of  $\mu$ , meaning that the hierarchical networks for different  $\mu$ 's are topologically similar as well.

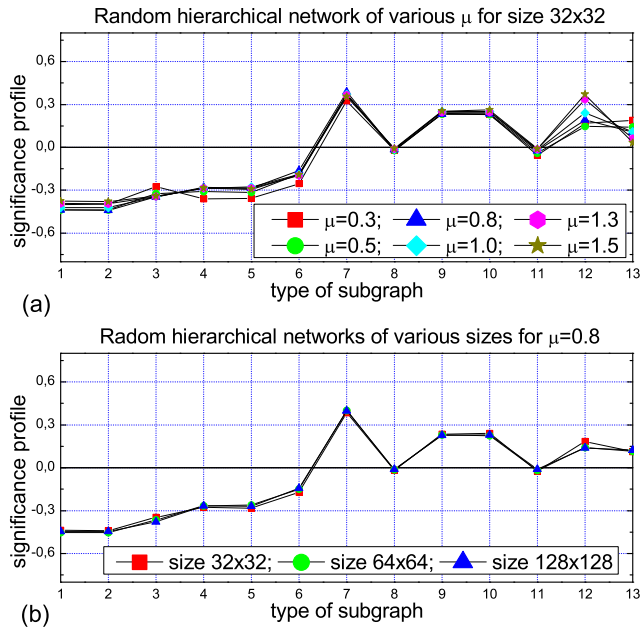


Figure 4: a) (Color online) Normalized motifs distribution for hierarchical 2-adic random network of size  $32 \times 32$  for different  $\mu$  (see the text for details); b) Normalized motifs distribution for hierarchical 2-adic random network of different sizes for single fixed value  $\mu = 0.8$ .

Comparing our distribution of motifs for directed hierarchical networks depicted in Fig.4 with the “second superfamily” in the classification of U. Alon *et al* shown in Fig.2 (look [11] for more details), one sees that in a broad range of  $\mu$ 's our directed hierarchical networks clearly fall into the “second superfamily”, to which, for example, the neuron networks belong.

We would like to emphasize that the hierarchical directed networks is, apparently, the first example of “hand-made” artificial networks topologically similar to a certain superfamily of natural networks in terms of local topological properties. We should stress that hierarchical random networks can be built by uncorrelated generation of clusters of links, unlike the essentially correlated preferential attachment procedure. In the light of results obtained, this feature looks particularly interesting in the context of modelling of biological operational systems and their evolutionary prototypes (e.g. [12]). From this point of view the hierarchical networks could be of particular interest for neuron networks modelling.

## B. Phase transition

We have checked our distribution of motifs (Fig.4) of directed hierarchical network on the stability. To study this question, the following numerical experiment has been performed. First, we have generated the block-hierarchical adjacency matrix of some directed graph, and then we randomly spoiled this block-hierarchical structure by the following procedure.

To be precise, we scanned *once* all matrix elements of the adjacency matrix row-by-row from the first element,  $a_{11}$ , to the last one,  $a_{NN}$ . Each element  $a_{ij}$  we have independently *switched* to the opposite value with the probability  $f$ , i.e. if  $a_{ij} = 1$ , then with the probability  $f$  the element  $a_{ij}$  can take the value 0 and vis versa. Obviously, for the noise  $f = 1/2$  after one run over all matrix elements, we have destroyed all hierarchical blocks and have generated a completely random adjacency matrix corresponding to the Erdős-Rényi random graph [13] with an appropriate distribution of motifs. Since our motifs' distribution is measured off the distribution of random uncorrelated graphs, the corresponding significance profile shown in Fig.4 would be definitely 0 for  $f_{up} = 1/2$  for all 13 configurations of triads.

To characterize quantitatively the degree of similarity between motifs' distributions for different  $f$ , we define the scalar product,  $\eta(f)$ :

$$\eta(f) = \mathbf{p}(f) \mathbf{p}(0) = \sum_{k=1}^{13} p_k(f) p_k(0) \quad (8)$$

where  $\mathbf{p}(f)$  is the distribution of motifs for a given value  $f$  of the noise, and  $\mathbf{p}(0)$  is the reference (initial) distribution of motifs for  $f = 0$ . The value  $\eta$  serves as an “order parameter” and its critical behavior is shown in the Fig.5 for three different sizes of networks  $32 \times 32$ ,  $64 \times 64$  and  $128 \times 128$ .

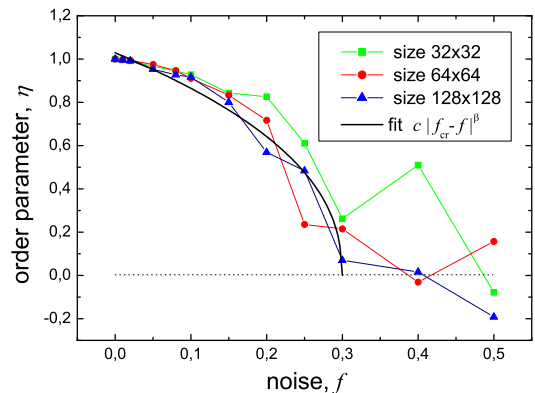


Figure 5: (Color online) Signature of the phase transition in distribution of motifs.

Varying the “intensity of noise”,  $f$ , from  $f = 0$  up to  $f_{up} = 1/2$ , we have noticed that the order parameter  $\eta$

becomes statistically indistinguishable from 0 for values of  $f$  significantly less than  $f_{\text{up}} = 1/2$ . Namely assuming the critical behavior

$$\eta(f) = c|f_{\text{cr}} - f|^\beta \quad (9)$$

we have found the following numerical values  $c \approx 1.72$ ;  $f_{\text{cr}} \approx 0.3$ ;  $\beta \approx 0.43$  for the best fit of the data corresponding the matrix of size  $128 \times 128$ . We can interpret this behavior as a signature of a possible phase transition characterized by the behavior of the order parameter  $\eta(f)$  in the block-hierarchical networks in the thermodynamic limit.

In order to demonstrate that the existence of the phase transition at finite temperature is very natural for the hierarchical system, we consider in the Appendix the toy model of the spin system on a complete graph with block-hierarchical coupling known in the literature as a ‘‘Dyson hierarchical model’’ [14, 15]. The method used here is based on the so-called  $p$ -adic Fourier transformation (see, for example [16] for details) and allows to re-derive the classical results on Dyson model in few lines.

The physical meaning of the hierarchy of phase transition in the hierarchical model discussed in the Appendix A is very clear. When the temperature decreases, at first critical temperature,  $T_{\text{cr}}^{(1)}$ , the spins become correlated within the smallest clusters only, where the interaction is the most strong. However, the clusters of 2nd and higher levels of hierarchy remain still uncorrelated because the interaction of spins inside them is weaker. At the second critical temperature,  $T_{\text{cr}}^{(2)}$  ( $T_{\text{cr}}^{(2)} < T_{\text{cr}}^{(1)}$ ) the smallest clusters remain correlated, together with the clusters of the 2nd hierarchical level, but the spins of the 3rd and higher level of hierarchy remain uncorrelated, and so on. Thus, approaching zero temperature is attended by a hierarchy of phase transition, along which larger and larger clusters of spins become correlated. Note that the application of the spin-glass models to networks (see, for example, [17]) suggests the opposite behavior, i.e. approaching zero temperature is attended by extension of correlations from larger to smaller clusters of the network nodes. In this respect, the hierarchical networks may constitute an alternative approach to modelling of natural networks.

#### IV. CONCLUSION

We have shown that the distribution of motifs in random hierarchical networks defined by nonsymmetric random block-hierarchical adjacency matrices coincides with the distribution of motifs in the second superfamily in the classification of U. Alon *et al* of networks [11] to which the class of neuron networks belongs. We would like to emphasize that apparently, this is the first example of ‘‘handmade’’ networks with the distribution of

motifs as in a special class of natural networks of essential biological importance.

Let us point out two important features of hierarchical networks constructed in our paper. First of all, any sub-graph belonging to a particular hierarchy level is an independent graph because the formation of clusters of links on each hierarchy level is entirely uncorrelated. Secondly, the sub-graphs, associated with different hierarchy levels of the network, can be different, so the network as a whole can be essentially nonuniform. In nature, the random graphs of such a hierarchical genesis can be encountered among the networks whose origins are associated with random events with low correlation, occurring with short evolutionary memory. The construction of such networks in some sense is very ‘‘simple’’, ‘‘rough’’ and ‘‘stable’’ because it does not demand a ‘‘fine tuning’’ of parameters to demonstrate the desirable properties (for example, the distribution of motifs). In particular, the networks of hierarchical genesis may be interesting as regards prebiology or the earliest biology.

We believe that our result could shed the light on the relation between the distribution of motifs and the structure of the adjacency matrix of a hierarchical network. However to make this relation more profound the ‘‘inverse’’ problem should be considered as well. Namely, it would be desirable to check if the stable distribution of motifs is uniquely related to any kind of hierarchical organization of the network. The result of our work concerning the critical behavior of motifs’ distribution on the noise intensity may be considered as a step towards this direction. This result demonstrates that the motifs’s distribution for hierarchical network has a ‘‘basin of stability’’ below some critical value  $f_{\text{cr}}$  of random perturbation of the hierarchical network.

We are guided by a general conjecture that the motifs distributions corresponding to four superfamilies of U. Alon *et al* could signalize the existence of islands of stability (attractors) in a sea of possible motifs’ distributions. Whether this conjecture is true or not we hope to see in the close future.

#### Acknowledgments

The authors are grateful to A. Mikhailov for paying our attention to motifs distribution and to M. Tamm and G. Kucherov for useful stimulating discussions. This work has been partially supported by the Program No. 24 of the Presidium of the Russian Academy of Sciences and by the ERARSysBio Plus grant #66.

### Appendix A: Phase transition in hierarchical spin system in an external field

In order to demonstrate that the existence of the phase transition is very natural in a hierarchical system, we consider the toy model of Ising spin system with symmetric block-hierarchical matrix of coupling constants. This model is known as ‘‘Dyson hierarchical model’’ [14, 15]. We outline the standard derivation of the mean-field solution of a spin system and discuss briefly the obtained results for our specific hierarchy of coupling constants.

Define the partition function  $Z$  of one-dimensional Ising spin chain with an arbitrary matrix  $U$  of coupling constants  $u_{ij}$

$$Z = \sum_{\{s_1, \dots, s_N\}} e^{\frac{1}{T} \sum_{ij} u_{ij} s_i s_j + \sum_{i=1}^N h_i s_i} \quad (\text{A1})$$

The spins  $s_i$  ( $i = 1, \dots, N$ ) take the values  $\pm 1$  and  $h_i$  is the external field acting on the spin  $s_i$ . Using the Hubbard-Stratonovich transform

$$e^{\frac{1}{T} \sum_{ij} u_{ij} s_i s_j} = \frac{\pi^{-N/2}}{\sqrt{\det U}} \int_{-\infty}^{\infty} \prod_{i=1}^N dx_i e^{-4T \sum_{ij} w_{ij} x_i x_j + \sum_{i=1}^N s_i x_i} \quad (\text{A2})$$

where  $w_{ij}$  is the element  $ij$  of the matrix  $W = U^{-1}$  and substituting (A2) into (A1), we can integrate over all spin configurations. The partition function  $Z$  reads now

$$Z = \frac{2^N}{\sqrt{\pi^N \det U}} \int_{-\infty}^{\infty} \prod_{i=1}^N dx_i e^{-TF(x_1, \dots, x_N)} \quad (\text{A3})$$

where

$$F(x_1, \dots, x_N) = 4 \sum_{ij} w_{ij} x_i x_j - \frac{1}{T} \sum_{i=1}^N \ln \cosh(x_i + h_i) \quad (\text{A4})$$

We evaluate (A3)–(A4) in the saddle-point (mean-field) approximation. The partition function of the system is  $Z = \exp\{-TF(x_1^{(0)}, \dots, x_N^{(0)})\}$  with  $F(x_1^{(0)}, \dots, x_N^{(0)})$  given by (A4) with  $x_i$  being the solutions of the equations  $\left. \frac{\partial F}{\partial x_i} \right|_{x_i=x_i^{(0)}} = 0$ . Setting the relation between vectors  $\mathbf{x}^{(0)} = \{x_1^{(0)}, \dots, x_N^{(0)}\}$  and  $\mathbf{y}^{(0)} = \{y_1^{(0)}, \dots, y_N^{(0)}\}$ :  $\mathbf{y}^{(0)} = U^{-1} \mathbf{x}^{(0)}$ , we get:

$$4y_i^{(0)} = \frac{1}{T} \tanh \left( \sum_{j=1}^N u_{ij} y_j^{(0)} + h_i \right) \quad (\text{A5})$$

For small arguments of  $\tanh(\dots)$  in the r.h.s. of (A5) one can linearize (A5) and rewrite it as

$$\sum_{j=1}^N (u_{ij} - 4T \delta_{ij}) y_j^{(0)} + h_i = 0 \quad (\text{A6})$$

Suppose now that the matrix of coupling constants  $U = \{u_{ij}\}$  has the block-hierarchical structure identical to the structure of the Parisi matrix  $A$  shown in Fig.3. For simplicity we consider the matrix elements of  $A$  to be nonrandom with  $a_\gamma^{(n)} = b_\gamma^{(n)} = 2^{-(\alpha+1)\gamma}$ , and the external field uniform  $h_i = h$  for all  $i \in [1, N]$ .

The solution of (A6) can be found using the methods of mathematical analysis on the field of  $p$ -adic numbers  $Q_p$ . This technique is based on parametrization of the matrix elements  $\{u_{ij}\}$  by the pairs of rational numbers  $\{z_i, z_j\}$  (see [18, 19]) by such a way that the  $p$ -adic norm  $|z_i - z_j|_p = p^{\gamma(z_i, z_j)}$  induces block-hierarchical structure of the matrix  $U = \{u_{ij}\}$  and therefore the coupling constants  $u_{ij}$  can be represented by an appropriate (real-valued) function  $u_{ij} = \rho(|z_i - z_j|_p) = a_{\gamma(z_i, z_j)}$ . In our case,  $\rho(|z_i - z_j|_p)$  is chosen in the form:

$$\rho(|z_i - z_j|_p) = \begin{cases} 0, & \gamma(z_i, z_j) \leq 0 \\ 2^{-(\alpha+1)\gamma(z_i, z_j)}, & \gamma(z_i, z_j) > 0 \end{cases} \quad (\text{A7})$$

Now, replacing the vector  $\mathbf{y}^{(0)} = \{y_1^{(0)}, \dots, y_N^{(0)}\}$  by the function  $f(z_i) = y_i^{(0)}$ , we can read (A6) as follows:

$$\sum_{j=1}^N \rho(|z_i - z_j|_p) f(z_j) - 4T f(z_i) + h = 0 \quad (\text{A8})$$

Continuous analog of Eq.(A8) in the thermodynamic limit  $N \rightarrow \infty$  is

$$\int_{Q_p} \rho(|z - z'|_p) \varphi(z) d_p z' - 4T \varphi(z) + h = 0, \quad (\text{A9})$$

where  $z \in Q_p$  and  $d_p z$  is the Haar measure on  $Q_p$ . Thus Eq.(A8) is understood as a discrete form of the  $p$ -adic equation (A9) induced by the relations  $\int_{|z-z_i|_p \leq 1} \varphi(z) d_p z = f(z_i)$  in the coset space  $Q_p/Z_p$ .

The solution of Eq.(A9) is easily found using the  $p$ -adic Fourier transformation (see, for example, [16]). In terms of the Fourier transforms  $\tilde{\varphi}(k)$  and  $\tilde{\rho}(|k|_p)$  of the functions  $\varphi(z)$  and  $\rho(|z - z'|_p)$ , Eq.(A9) looks as

$$\tilde{\rho}(|k|_p) \tilde{\varphi}(k) - 4T \tilde{\varphi}(k) + h = 0 \quad (\text{A10})$$

giving the solution

$$\tilde{\varphi}(k) = \frac{h}{4T - \tilde{\rho}(|k|_p)} \quad (\text{A11})$$

The function  $\tilde{\varphi}(k)$  has the poles at the set of critical temperatures  $T_{\text{cr}}$ , determined by the equation

$$4T_{\text{cr}} - \tilde{\rho}(|k|_p) = 0$$

The values of  $T_{\text{cr}}$  can be easily determined in the closed form by knowing that

$$\tilde{\rho}(|k|_p) = \begin{cases} 0, & |k|_p > 1 \\ \Gamma_p(-\alpha) |k|_p^\alpha + A_\alpha, & |k|_p \leq 1 \end{cases} \quad (\text{A12})$$

where  $\Gamma_p(-\alpha) = \frac{1-p^{-(\alpha+1)}}{1-p^{-\alpha}}$  is the  $p$ -adic  $\Gamma$ -function and  $A_\alpha = (1-p^{-1})\frac{p^{-\alpha}}{1-p^{-\alpha}}$ .

Since the Fourier transform (A12) of the function  $\rho(|z-z'|_p)$  given by (A7) possess discrete values  $|k|_2^\alpha = 2^{-\alpha\gamma}$ ,  $\gamma = 0, 1, 2, \dots$ , the system of hierarchically interacting Ising spins has a hierarchy of critical temperatures

$$T_{\text{cr}}^{(\gamma)} = \tilde{\rho}(2^{-\alpha\gamma})/4 \quad (\text{A13})$$

It should be noted that in fact the hierarchy of critical temperatures  $T_{\text{cr}}^{(\gamma)}$  defined by (A12)–(A13) exist only for  $\alpha > 0$ . As soon as  $\alpha \rightarrow 0$  the intervals between  $T_{\text{cr}}^{(\gamma)}$  tend to zero and the hierarchical model becomes similar to ordinary mean-field ferromagnetic system without the hierarchy of interactions.

- 
- [1] A. Y. Grosberg, S. K. Nechaev and E. I. Shakhnovich, J. Phys. (Paris) **49**, 2095 (1988)
- [2] B. Mandelbrot, *The Fractal Geometry of Nature*, (New York: W.H. Freeman and Co., 1982)
- [3] V. A. Avetisov, A. V. Chertovich, S. K. Nechaev, and O. A. Vasilyev, J. Stat. Mech: Theory and Exper. **07** 07008 (2009);
- [4] V. A. Avetisov, A. Kh. Bikulov, O. A. Vasilyev, S. K. Nechev, and A. V. Chertovich, JETP, **109(3)** 485 (2009)
- [5] M. Mezard, G. Parisi, M. Virasoro, *Spin glass theory and beyond* (World Scientific: Singapore, 1987)
- [6] I.J. Farkas, I. Derényi, A.-L. Barabási, T. Vicsek, Phys. Rev. E **64** 026704 (2001)
- [7] K.-I. Goh, B. Kahng, D. Kim, Phys. Rev. E **64** 051903 (2001)
- [8] R. Albert and A.-L. Barabási, Rev. Mod. Phys., **74** 47 (2002)
- [9] A.-L. Barabási and R. Albert, Science **286** 509 (1999); A.-L. Barabási, R. Albert, H. Jeong, Physica A **272** 173 (1999); A.-L. Barabási, R. Albert, H. Jeong, Physica A **281** 69 (2000)
- [10] R. Milo, S. Shen-Orr, S. Itzkovitz, N. Kashtan, D. Chklovskii, U. Alon, Science **298** 824 (2002)
- [11] R. Milo, Sh. Itzkovitz, N. Kashtan, R. Levitt, Sh. Shen-Orr, I. Ayzenshtat, M. Sheffer, U. Alon, Science, **303** 1538 (2004)
- [12] Yu. I. Wolf, E. V. Koonin, Biology Direct **2** 14 (2007)
- [13] P. Erdős, A. Rényi, Publ. Math. Inst. Hung. Acad. Sci. Ser. A **5** 17 (1960)
- [14] F.J. Dyson, Comm. Math. Phys. **12** 91 (1969)
- [15] G.A. Baker Jr., Phys. Rev. B **5** 2622 (1972)
- [16] V. S. Vladimirov, I. V. Volovich, E. I. Zelenov *p-Adic Analysis and Mathematical Physics* (Singapore: World Scientific, 1994)
- [17] V. Dotsenko *An Introduction to the Spin Glasses and Neural Networks* (Singapore: World Scientific, 1994)
- [18] V. A. Avetisov, A. Kh. Bikulov, S. V. Kozyrev, J. Phys. A: Math. Gen. **32** 8785 (1999)
- [19] G. Parisi, N. Sourlas, Eur. J. Phys. B **14** 535 (2000) 063302 (2005)